

Acoustic velocities, refractive index, and elastic constants of liquid and solid CO₂ at high pressures up to 6 GPa

H. Shimizu, T. Kitagawa, and S. Sasaki

Department of Electronics and Computer Engineering, Gifu University, 1-1 Yanagido, Gifu 501-11, Japan

(Received 21 January 1993)

Acoustic velocities, refractive index, and elastic constants of liquid and solid CO₂ have been determined at pressures up to 6 GPa by applying Brillouin spectroscopy developed for condensed gases in a diamond-anvil high-pressure cell. The analyses of the angular dependence of Brillouin acoustic velocities show that the solid CO₂ remains in the cubic (dry ice) phase I throughout the range of pressure from freezing (0.6 GPa) to 6 GPa at 300 K.

I. INTRODUCTION

The high-pressure behavior of carbon dioxide (CO₂) is of fundamental importance in condensed-matter physics and planetary sciences. There is considerable uncertainty about high-pressure solid phases: The indication for phase II between 0.5 and 2.3 GPa at 300 K (Ref. 1) could not be verified in further x-ray² and Raman^{3,4} studies, and the evidence for a phase IV above 5 GPa (Refs. 4 and 5) is puzzling. Data on acoustic and elastic properties of CO₂ in this pressure range have been lacking.

In this paper, we present determinations of acoustic velocities, refractive index, polarizability, and elastic constants of liquid and solid CO₂ up to 6 GPa by using Brillouin scattering measurements⁶ for the angular dependence of acoustic velocities with *in situ* identification of the orientation of the single crystal grown in a diamond-anvil cell (DAC). From these results, we investigate the high-pressure solid phases to clarify the pressure-temperature phase diagram of CO₂.

II. THEORETICAL BASICS

From the Brillouin equation for the cubic system, Every⁷ derived the relation between sound velocities for arbitrary directions and elastic constants. The ρv_j^2 is expressed as a function of six parameters as follows:

$$\rho v_j^2 = f_j(C_{11}, C_{12}, C_{44}, q_x, q_y, q_z), \quad (1)$$

where ρ is the density, subscript j ($=0, 1, 2$) indicates LA, TA₁ (slow), and TA₂ (fast) modes, respectively, and q_x , q_y , and q_z are direction cosines of the phonon. For the application of these results to our experimental system, we set up the geometrical relation of Cartesian coordinates: Euler angles (θ, ϕ, χ) relate the laboratory frame (X, Y, Z) to the crystal reference frame (x, y, z) . The v_j therefore can be expressed as a function of six parameters,

$$v_j = g_j(C_{11}/\rho, C_{12}/\rho, C_{44}/\rho, \theta, \phi, \chi), \quad (2)$$

where

$$q_x = \cos\theta \cos\phi \cos\chi - \sin\phi \sin\chi,$$

$$q_y = -\cos\theta \cos\phi \sin\chi - \sin\phi \cos\chi,$$

and $q_z = \sin\theta \cos\phi$. In order to determine the three Euler angles and three elastic constants at each pressure, we applied a computerized least-squares fit between calculations $g_j(\phi_i)$ and experimental velocities (ϕ_i, v_{ji}) as a function of angle ϕ_i ,

$$J = \sum_{ij} [g_j(\phi_i) - v_{ji}]^2 \quad (j=0, 1, 2), \quad (3)$$

where J is minimized by systematically varying the six parameters until the fit is optimized. As a result, we can determine the crystal orientation (θ, ϕ, χ) and the acoustic velocities for arbitrary directions.

III. EXPERIMENT

Gaseous CO₂ condenses directly to the solid phase I (dry ice; space group, $Pa3$) at 194.5 K and 1 bar, and to liquid CO₂ in the vicinity of 75 bar at 300 K. For loading CO₂ samples in the DAC, we condensed gaseous CO₂ by spraying its vapor into the gasket hole (diameter, 0.3 mm; depth, 0.2 mm) of the DAC cooled in liquid nitrogen, where the surrounding in the vessel had been already replaced by the N₂ gas⁸ to protect the sample from contaminations. After adequate pressure had been applied, the DAC was warmed to 300 K. A transparent single-crystal was grown by increasing the pressure on a seed crystal, which coexists with the liquid CO₂ at about 0.6 GPa. Pressures were measured by the ruby-scale method.⁹

For Brillouin scattering measurements, the 514.5-nm argon-ion laser line (λ_0) with a single mode was used. The heart of the apparatus was a plane piezoelectrically scanned Fabry-Pérot interferometer, which was used in a five-pass configuration.¹⁰

The Brillouin frequency shifts ($\Delta\nu$) at 90° and 180° (angles between the incident and the scattered beams) scattering geometries with the DAC are related to the acoustic velocities as follows:¹¹

$$\Delta\nu_{90} = \sqrt{2}v_{90}/\lambda_0, \quad (4)$$

$$\Delta\nu_{180} = (2n)v_{180}/\lambda_0, \quad (5)$$

where the wave vector \mathbf{q} of probed acoustic phonons is parallel (90°) and perpendicular (180°) to interfaces of the input and output diamonds crossed by the laser beam,

and v_{90} is independent of the refractive index (n) of the medium.

IV. RESULTS AND DISCUSSION

For the liquid CO₂ at pressures up to 0.6 GPa and 300 K, the pressure dependence of acoustic velocity was determined from the observed Brillouin shifts at 90° scattering [Eq. (4)], which is shown in Fig. 1. The velocity increases sharply with pressure. Near 75 bar (close to zero in Fig. 1), the present sound velocity indicates 0.31 km s⁻¹, which is comparable to the values determined by Brillouin studies around the critical point of CO₂.¹² Because the liquid is acoustically isotropic, the velocity is the same for any direction. There is also a laser beam reflected from the output diamond that serves as incident light, giving the 180° scattering signal.^{11,13} Both Δv_{90} and Δv_{180} could be detected simultaneously, and therefore we determined the pressure dependence of n by using the ratio of Δv_{90} to Δv_{180} , $\Delta v_{90}/\Delta v_{180} = 1/(\sqrt{2}n)$ (solid circles in Fig. 2). n increases sharply with pressure and has, near the solidification point, the value of about 1.35 which is comparable to that of H₂O at 1 bar. Near 75 bar (close to zero in Fig. 2), the refractive index indicates $n=1.19$, which is comparable to the values used for Brillouin studies around the critical point of CO₂.^{12,14}

For the solid CO₂ at pressures between 0.6 and 6 GPa, the acoustic and elastic properties have been studied by using the method of high-pressure Brillouin spectroscopy recently developed for simple molecular solids.⁶ Brillouin measurements at 90° scattering geometry were made in 10° intervals of rotation angle ϕ about the load axis of DAC in the laboratory frame. The observed Brillouin shifts, that is, acoustic velocities at 1.92 GPa, are plotted as a function of ϕ as open circles in Fig. 3. The computerized least-square fit was applied to determine elastic constants and Euler angles (orientation of CO₂ single-crystal grown in the DAC). The best-fit calculations are represented by dotted lines in Fig. 3. There are excellent agreements between the measured and the fitted values, which yielded, for example, $C_{11}/\rho = 12.43$, $C_{12}/\rho = 7.88$, and $C_{44}/\rho = 4.37$ GPa cm³ g⁻¹ at 1.92 GPa. These best-fit results strongly indicate that the pressure-induced

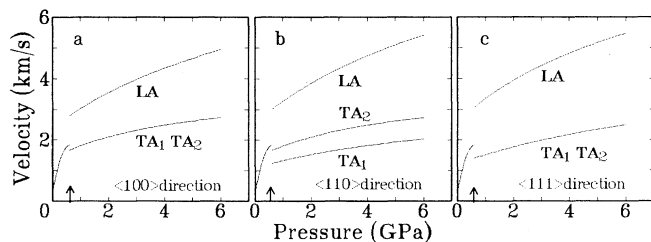


FIG. 1. The pressure dependence of acoustic velocities for liquid and solid CO₂ at 300 K. Vertical arrows indicate the liquid-solid phase transition point (0.6 GPa). In the solid phase, the velocities for typical directions are shown: (a) $\langle 100 \rangle$, (b) $\langle 110 \rangle$, and (c) $\langle 111 \rangle$ directions. LA, TA₁, and TA₂ are longitudinal, and slow and fast transverse modes, respectively.

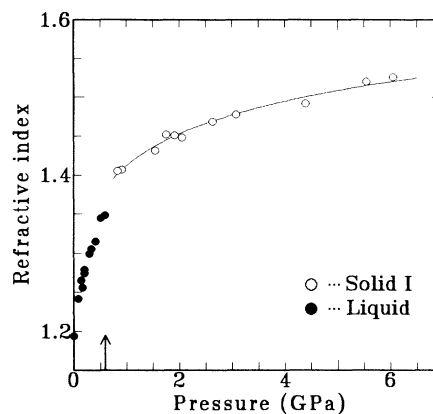


FIG. 2. The pressure dependence of the refractive index (n) for liquid and solid CO₂ at 300 K. Vertical arrow indicates the liquid-solid phase transition point (0.6 GPa). Solid circles, liquid; open circles, solid I. Solid line is fitted by $n = 1.41 \times P^{0.041}$, where P is in GPa.

solid phase at 300 K belongs to the cubic phase I ($Pa\bar{3}$). It has turned out from the identification of the crystal orientation (θ, ϕ, χ) and its pressure dependence that (1) the CO₂ single crystal grows every time with a different orientation relative to the cell axis, and (2) the crystal orientation changes gradually in the DAC with pressure, that is, the uniaxial-stress component in the DAC increases gradually with increasing pressure. We did not observe the phenomenon of the sudden crystal reorientation as reported on crystalline Ar in the DAC at high pressures.^{15,16}

Once the six parameters were determined, the acoustic velocities could be calculated for all directions. Figure 1 shows the CO₂ sound velocities for typical directions as a function of pressure up to 6 GPa. At the freezing point, sound velocity shows discontinuous changes to LA, TA₁, and TA₂ in the solid phase I, which increase with pressure. Furthermore, we can calculate the sound velocity (v_{180}) along the direction perpendicular to the diamond

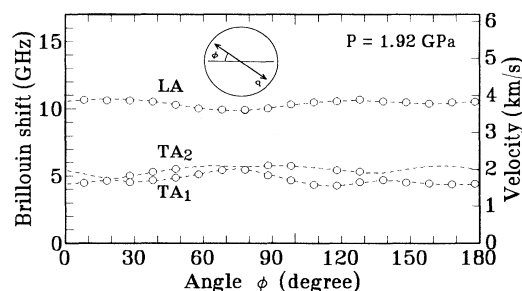


FIG. 3. Brillouin frequency shifts and acoustic velocities of LA, TA₁, and TA₂ modes as a function of angle ϕ at a 90° scattering geometry for solid CO₂ at 1.92 GPa. Open circles indicate experimental points, and the dotted lines represent the calculated best fit velocities. The circled inset shows the rotation angle ϕ about the load axis of DAC.

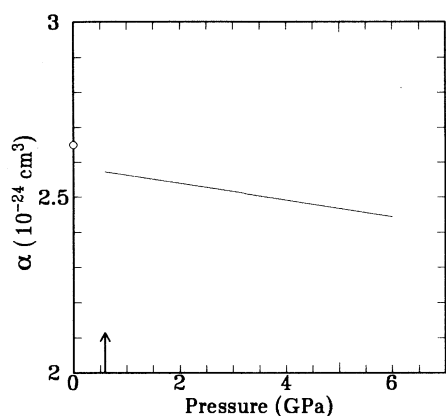


FIG. 4. The pressure dependence of polarizability α for solid CO_2 at 300 K. Open circle at 1 bar shows the value of gaseous CO_2 . Vertical arrow indicates the solidification point (0.6 GPa).

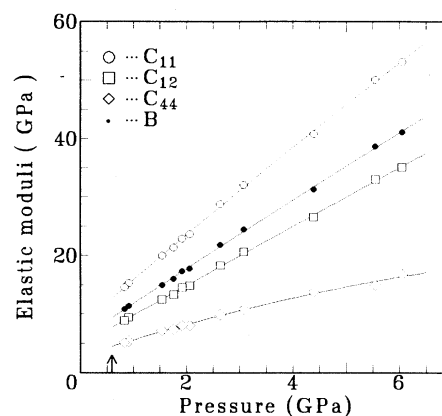


FIG. 5. The pressure dependence of elastic constants C_{11} , C_{12} , and C_{44} , and the adiabatic bulk modulus $B [(C_{11} + 2C_{12})/3]$ for the solid CO_2 at 300 K. Vertical arrow indicates the solidification point (0.6 GPa).

interfaces, which is available to determine n by using Eq. (5). From Δv_{180} measured at 180° scattering geometry, we can obtain the pressure dependence of n as shown in Fig. 2. At the liquid-solid phase transition point, n shows a discontinuous increase of about 4% and, moreover, increases gradually with pressure up to $n=1.53$ at 6 GPa. A solid line in Fig. 2 is fitted by the equation, $n = 1.41 \times P^{0.041}$ ($P \geq 0.6$ GPa) with P in GPa. From these results and the pressure dependence of ρ by the x-ray studies,² the Lorentz-Lorenz relation $(n^2 - 1)/(n^2 + 2) = 4\pi N \rho \alpha / 3M$ yields the polarizability α , where N is Avogadro's number, and M is the molecular weight. Figure 4 shows the pressure dependence of the α in the solid phase; its value is $2.56 \times 10^{-24} \text{ cm}^3$ at 1 GPa and decreases with pressure to $2.44 \times 10^{-24} \text{ cm}^3$ at 6 GPa. This decrease can be understood as follows: CO_2 molecules are compressed and become harder to deform or displace at these pressures.

Figure 5 shows the pressure dependence of elastic constants C_{11} , C_{12} , and C_{44} , and the adiabatic bulk modulus $B [(C_{11} + 2C_{12})/3]$, which were determined from the best fitted results of C_{ij}/ρ with the pressure dependence of ρ from x-ray studies.² Then, the degree of elastic anisotropy given by $A = 2C_{44}/(C_{11} - C_{12})$ is about 1.9 at 1.92 GPa, and it is almost independent of pressure. Recently, the pair-potential rigid-molecule approximation has been applied to calculate theoretically the elastic constants of solid CO_2 ,¹⁷ $C_{11} = 12.34$, $C_{12} = 7.01$, and $C_{44} = 5.51$ GPa at low pressure. Our results are, for ex-

ample, $C_{11} = 12.84$, $C_{12} = 7.80$, and $C_{44} = 4.53$ GPa at 0.6 GPa, which are fairly comparable to the calculations. The present experimental results will therefore motivate some theoretical model calculations in the field of molecular dynamics.

Finally, we investigate pressure-induced phase transitions in solid CO_2 . Neither the present high-pressure Brillouin studies nor optical observations by a microscope could detect any change caused by a phase transition at pressures below 6 GPa. Above 6 GPa, however, the computerized least-squares fit between calculations and experimental velocities as a function of angle ϕ could not be perfectly accomplished, and this tendency accelerates with increasing pressure. This behavior at higher pressures is probably due to a change in experimental conditions for the truly hydrostatic pressure in the CO_2 cubic phase. The present experimental observation above 6 GPa may correspond to the existence of the new phase IV above 5 GPa which was suggested by Raman measurements,⁴ and ascribed to the uniaxially stressed instability.⁴ However, we cannot interpret this phenomenon as caused by a phase transition, because this observation depends on the hydrostatic condition for the applied high pressures in the DAC. At present we conclude that the solid CO_2 remains in the normal cubic phase I up to at least 6 GPa. This is consistent with the results of x-ray studies by Olinger² and Raman studies by Hanson.³

¹L. Liu, *Nature (London)* **303**, 508 (1983).

²B. Olinger, *J. Chem. Phys.* **77**, 6255 (1982).

³R. C. Hanson, *J. Phys. Chem.* **89**, 4499 (1985).

⁴H. Olijnyk, H. Dauffer, H. J. Jodl, and H. D. Hochheimer, *J. Chem. Phys.* **88**, 4204 (1988).

⁵B. Kuchta and R. D. Etters, *Phys. Rev. B* **38**, 6265 (1988).

⁶H. Shimizu and S. Sasaki, *Science* **257**, 514 (1992).

⁷A. G. Every, *Phys. Rev. Lett.* **42**, 1065 (1979).

⁸H. Shimizu, Y. Nakamichi, and S. Sasaki, *J. Chem. Phys.* **95**, 2036 (1991).

⁹F. D. Barnett, S. Block, and G. J. Piermarini, *Rev. Sci. Instrum.* **44**, 1 (1973).

¹⁰S. Sasaki, S. Katoh, and H. Shimizu, *Jpn. J. Appl. Phys.* **31** (Supplement 31-1), 17 (1992).

¹¹H. Shimizu, E. M. Brody, H. K. Mao, and P. M. Bell, *Phys. Rev. Lett.* **47**, 128 (1981).

- ¹²R. W. Gammon, H. L. Swinney, and H. Z. Cummins, *Phys. Rev. Lett.* **19**, 1467 (1967).
- ¹³E. M. Brody, H. Shimizu, H. K. Mao, P. M. Bell, and W. A. Bassett, *J. Appl. Phys.* **52**, 3583 (1981).
- ¹⁴N. C. Ford, K. H. Langley, and V. G. Puglielli, *Phys. Rev. Lett.* **21**, 9 (1968).
- ¹⁵P. M. Bell and H. K. Mao, *Carnegie Inst. Washington Yearb.* **80**, 404 (1981).
- ¹⁶M. Grimsditch, P. Loubeyre, and A. Polian, *Phys. Rev. B* **33**, 7192 (1986).
- ¹⁷P. Pavlides, D. Pugh, and K. J. Roberts, *Mol. Phys.* **72**, 121 (1991).